

TRIAXIAL HIGH TEMPERATURE MECHANICAL PROPERTIES OF LONGMAXI SHALE AT DIFFERENT DEPTHS

by

**Ze-Qian YANG^a, Hui-Jun LU^b, Ru ZHANG^{a,c}, Ze-Tian ZHANG^{a,c*},
Li REN^c, Lan-Bin ZHANG^a, and An-Lin ZHANG^a**

^a College of Water Resource and Hydro Power, Sichuan University, Chengdu, China

^b School of Architecture and Civil Engineering, Xihua University, Chengdu, China

^c MOE Key Laboratory of Deep Earth Science and Engineering,
Sichuan University, Chengdu, China

Original scientific paper

<https://doi.org/10.2298/TSCI2305817Y>

Based on the high temperature and confining pressure conditions at different depths, triaxial high temperature mechanical tests were carried out on Longmaxi shale with horizontal and vertical bedding, respectively. The results show that shale's peak strength and deformation capacity increase with burial depth. The failure mode of shale is a typical brittle failure, and the brittle index can quantitatively describe the brittle mechanical behavior of shale. Because shale has an apparent thin bedding structure, shale with different bedding directions shows pronounced anisotropy in mechanical parameters and deformation characteristics. The burial depth and bedding direction significantly impact the energy evolution law of Longmaxi shale during the mechanical process.

Key words: shale, different depths, bedding direction, mechanical properties, energy evolution

Introduction

The vast and bountiful shale gas resources in the Sichuan Basin have long been a source of fascination for geologists and engineers alike. Efficiently developing these deep shale gas resources requires a thorough understanding of critical technical aspects such as reservoir reconstruction and wellbore stability control [1, 2]. Deep in-situ high temperature and high confining pressure environment change the mechanical behavior of shale. At the same time, shale has an apparent bedding structure, and anisotropic characteristics make deep shale's damage and failure process more complex. Therefore, the triaxial high temperature mechanical test research of shale with different depths has guiding value for shale gas reservoir fracturing design and drilling stability control.

The study of the triaxial mechanical properties of shale has been a subject of intense interest among scholars, who have conducted many theoretical and experimental investigations. High temperature, confining pressure, and bedding direction are closely related to the deformation damage, crack propagation, and failure process of shale [3-5]. The anisotropic mechanical tests of oil shale at a high temperature reveal that the elastic modulus and compressive strength of vertical bedding oil shale undergo an initial decrease followed by an increase [6]. Similarly, a large number of shale mechanical test results indicate that the influence of bedding on the mechanical properties and failure characteristics of shale cannot be ignored [7-9]. Spe-

* Corresponding author, e-mail: zhangzetian@scu.edu.cn

cifically, the stratification plane affects the elastic modulus, failure mode, and energy release level of shale [10, 11]. However, the existing research rarely considers the influence of in-situ temperature and confining pressure conditions of deep shale reservoirs on the anisotropic mechanical behavior of shale simultaneously.

China's deep shale reservoir depth is mainly in the range of 2500-4500 m [12]. This study selected typical reservoir depths of 2000 m and 4000 m. High temperature triaxial mechanical tests were carried out on Longmaxi shale in two directions (horizontal bedding and vertical bedding) based on in-situ temperature and confining pressure conditions. The mechanical response law of Longmaxi shale is analyzed from mechanical parameters, brittleness index, deformation characteristics, and energy evolution. The research results can provide a theoretical data basis for developing deep shale gas resources.

Testing information

The test rock sample is Longmaxi shale in Chongqing, China. Standard rock samples (50 mm in diameter and 100 mm in height) were prepared from ISRM rock samples. Grind and polish rock samples to meet the requirements of indoor rock testing. The triaxial high temperature mechanical test equipment adopts the MTS 815 Flex Test GT rock mechanics test system of Sichuan University to carry out high temperature loading and stress-strain data collection.

The temperature and confining pressure control conditions during the test are determined according to the in-situ stress and temperature tests at the occurrence depth of 2000 m and 4000 m. The temperature corresponding to the depth of 2000 m is 73.49 °C, and the confining pressure is 42.64 MPa. The temperature corresponding to the depth of 4000 m is 102.7 °C, and the confining pressure is 89.15 MPa. During the test, the temperature is controlled at a heating rate of 12 °C per hour. After reaching the target temperature and stabilizing, load the confining pressure at 3 MPa per minute. Finally, the displacement control method is adopted to load the shale sample to failure, and the loading rate is 0.04 mm per minute.

Result and analysis

Stress-strain curves

Generally, the stress-strain curve of rock under triaxial stress has five classical stages [13]. According to the triaxial high temperature test of Longmaxi shale at different depths, the stress-strain curves of Longmaxi shale at different depths and bedding directions are obtained, as shown in fig. 1. Figures 1(a) and 1(b) correspond to 2000 m of horizontal and vertical bedding, while figs. 1(c) and 1(d) correspond to 4000 m. All naming methods follow this rule. In the initial crack compaction stage, the microcracks in the shale are closed, and the whole rock sample is compacted, showing a curve of gradual increase of axial stress and slow increase of strain. This stage is not evident because the rock sample is relatively dense and has low porosity. In the elastic deformation stage, the stress-strain curve increases approximately linearly, which can be used to measure the mechanical parameters such as elastic modulus and Poisson's ratio. In the stable crack growth stage, the initial stress point is the crack initiation stress. The micro-damage, weak cementation surface, and other low strength points in the shale initiate micro-cracks. The slope of the stress-strain curve decreases, and the rock sample produces non-linear plastic deformation. In the unstable crack development stage, the initial stress point is crack damage stress, and the volume strain of the rock reaches the maximum value. The micro-cracks in the shale gradually generated and began to form macro-cracks. The end stress point of this stage is peak stress. In the post-peak failure stage, macro cracks are rapidly generated. The bearing capacity of shale decreases rapidly, and apparent brittle failure occurs.

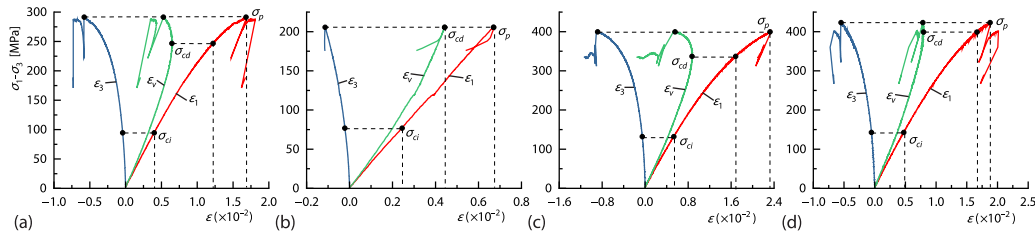


Figure 1. Stress-strain curves of Longmaxi shale; ϵ_1 – axial strain, ϵ_3 – lateral strain, and ϵ_v – volumetric strain

Mechanical parameters

Both elastic modulus, E , and Poisson's ratio, ν , are important mechanical parameters reflecting the deformation characteristics of rock materials. The mechanical parameters of Longmaxi shale at different depths and bedding directions are shown in tab. 1. The data of Lu *et al.* [14] were quoted at a depth of 3000 m in the study. For data comparison, the same mechanical parameter calculation method is used. The peak strength, σ_p , of shale increases with depth. However, the elastic modulus and Poisson's ratio show a non-linear trend. Therefore, studying deep rock mechanics should fully consider the influence of deep in-situ occurrence environment. As a layered rock, the deformation and strength properties of Longmaxi shale are anisotropic. The mechanical parameters of shale with two different bedding directions are compared. At the same depth, the elastic modulus of vertical bedding shale is greater than that of horizontal bedding shale.

Table 1. Mechanical parameters of Longmaxi shale with different depths and bedding directions

Depths [m]	Bedding directions	σ_p [MPa]	E [GPa]	ν
2000	Horizontal	333.99	22.10	0.17
	Vertical	248.15	30.66	0.13
3000 [14]	Horizontal	414.01	21.97	0.18
	Vertical	476.32	31.79	0.19
4000	Horizontal	488.62	21.73	0.19
	Vertical	512.12	27.79	0.18

Brittleness index

Rock materials exhibit a fundamental mechanical property called brittleness that governs their deformation and fracture behavior under stress. In shale gas production engineering, the brittle mechanical behavior of shale material constitutes a critical factor that regulates the fracture growth pattern and profoundly impacts the hydraulic fracturing effect. Consequently, evaluating shale brittleness is paramount for accurately assessing its mechanical behavior.

By understanding the aforementioned stress-strain curve, we can think that the unstable failure process of Longmaxi shale after the peak reflects the brittle deformation characteristics. The elastic modulus and Poisson's ratio of Longmaxi shale in the Sichuan basin are 8-56 GPa and 0.1-0.36, respectively [15, 16]. The brittleness index of Longmaxi shale at different depths and bedding directions is shown in fig. 2. With the increase of the occurrence depth of shale, the coupling effect of confining pressure, temperature, and loading stress makes the

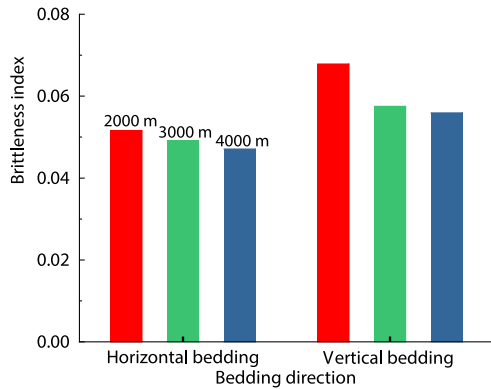


Figure 2. Brittleness index of Longmaxi shale at different depths and bedding directions

shale have the trend of transition from brittleness to ductility. At the same depth, the brittleness index of vertical bedding shale is greater than that of horizontal bedding shale.

Deformation characteristics

The comprehension of the deformation and brittle failure process of Longmaxi shale largely depends on its characteristic stress and anisotropic deformation characteristics under high temperatures at various depths. The crack damage stress, σ_{cd} , corresponding to the maximum point of volumetric strain is crack damage stress. The crack initiation stress, σ_{ci} , of Longmaxi shale is solved by the crack vol-

ume strain method [17]. According to the evolution law of crack volume strain, ε_v^c , the stress turning point at different deformation and failure stages is determined as the crack initiation stress. The crack initiation, damage, and peak stress, σ_p , points determined according to the volume and crack volume strain curves are shown in fig. 3.

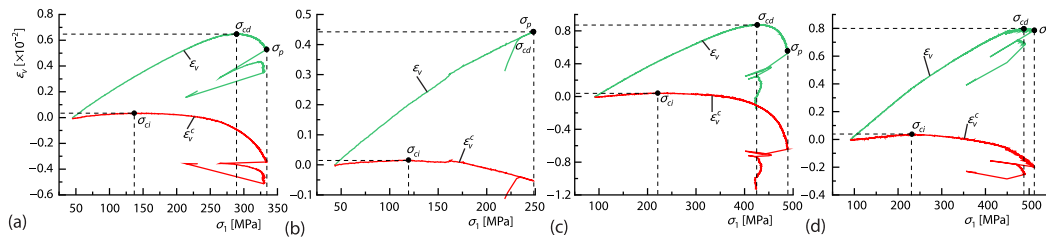


Figure 3. Stress-volumetric strain curves of Longmaxi shale

The deformation parameters and characteristic stress values of Longmaxi shale at different depths and bedding directions are shown in tab. 2. The analysis shows that the peak axial, lateral, and volumetric strain (ε_{1p} , ε_{3p} , ε_{vp}) increase with the increase of occurrence depth, and the deep shale shows more vital deformation ability than the shallow shale. The three peak strains of horizontal bedding shale are greater than those of vertical bedding shale. The deformation ability of vertical bedding shale is weak, showing strong brittleness. The change rule of crack initiation and damage stress with depth and bedding direction is the same as the peak strength. Since the crack damage stress at 2000 m equals the peak stress, the shale directly enters the post-peak failure stage from the stable crack growth stage. It is inferred from this phenomenon that vertical bedding affects the brittle failure of shale samples.

Table 2. Deformation parameters of Longmaxi shale with different depths and bedding directions

Depths [m]	Bedding direction	$\varepsilon_{1p} (\cdot 10^{-2})$	$\varepsilon_{3p} (\cdot 10^{-2})$	$\varepsilon_{vp} (\cdot 10^{-2})$	σ_{ci} [MPa]	σ_{cd} [MPa]
2000	Horizontal	1.81	-0.73	0.65	136.99	289.24
	Vertical	0.67	-0.12	0.44	119.46	248.05
4000	Horizontal	2.34	-1.13	0.87	221.19	426.14
	Vertical	2.01	-0.73	0.80	231.66	488.01

Energy evolution

The study of rock mechanics often involves analyzing the energy exchange that occurs during deformation and failure [18]. Assuming that there is no heat exchange between the shale and the outside during loading, according to the first law of thermodynamics, the total input energy generated by the external force work of the shale under triaxial stress can be calculated. The energy evolution curves of Longmaxi shale at different depths and bedding directions are shown in fig. 4. In the initial fracture compaction stage, the total input energy, elastic strain energy, and dissipated energy increase slowly. In the elastic deformation and stable crack growth stages, some energy is converted into elastic strain energy and stored in the shale, while the other part is dissipated in the form of plastic properties and damage energy. In the unstable crack growth stage, the growth rate of dissipated energy increases obviously, and the growth rate of elastic strain energy decreases accordingly. The elastic strain energy at the peak stress reaches the maximum value. Then it enters the post-peak failure stage of shale, and the elastic strain energy is suddenly released and converted into dissipated energy for shale damage and failure. At the peak stress level, the total input energy of Longmaxi shale in the shallow part is higher than that in the deep part; At the same depth, the total input energy of horizontal bedding Longmaxi shale is higher than that of vertical bedding.

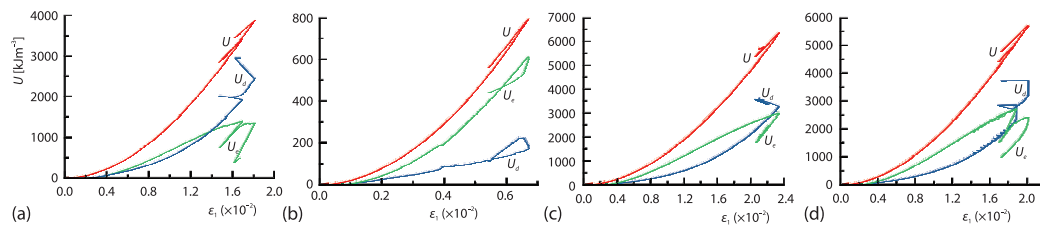


Figure 4. Energy evolution curves of Longmaxi shale at different depths and bedding directions

Conclusion

Different depths were selected for the mechanical properties tests of horizontal and vertical bedding Longmaxi shale, and the mechanical parameters, brittleness index, deformation characteristics, and energy evolution laws of shale in different depths were obtained. In the triaxial mechanical tests under different high temperatures, the peak strength of Longmaxi shale increases with the depth, while the elastic modulus and Poisson's ratio show a non-linear trend. As the occurrence depth increases, the Longmaxi shale exhibits stronger deformation characteristics. Additionally, the brittleness index of vertical bedding shale is greater than that of horizontal bedding shale. The deformation and failure process of Longmaxi shale is accompanied by regular energy input, dissipation, and release.

Acknowledgment

This research was funded by the National Natural Science Foundation of China (52125402) and the Natural Science Foundation of Sichuan Province, China (2022NSFSC0005).

Nomenclature

E – elastic modulus, [GPa]
 U – total input energy, [kJm^{-3}]
 U_d – dissipated energy, [kJm^{-3}]
 U_e – elastic strain energy, [kJm^{-3}]
 ν – poisson's ratio, [-]

Greek symbols

ε_1 – axial strain, [-]
 ε_3 – lateral strain, [-]
 ε_v – volumetric strain, [-]
 ε_v^c – crack volume strain, [-]

ε_{3p}	– peak lateral strain, [–]	σ_3	– confining pressure, [MPa]
ε_{1p}	– peak axial strain, [–]	σ_{ci}	– crack initiation stress, [MPa]
ε_{vp}	– peak volumetric strain, [–]	σ_p	– peak stress, [MPa]
σ_1	– axial stress, [MPa]	σ_{cd}	– crack damage stress, [MPa]

References

- [1] Zou, C., *et al.*, Shale Gas in China: Characteristics, Challenges and Prospects (II) (in Chinese), *Petroleum Exploration and Development*, 43 (2016), 2, pp. 182-196
- [2] Lu, H., *et al.*, Damage Characterization of Shale under Uniaxial Compression by Acoustic Emission Monitoring, *Frontiers of Earth Science*, 15 (2021), 4, pp. 817-830
- [3] Rybacki, E., *et al.*, Creep of Posidonia Shale at Elevated Pressure and Temperature, *Rock Mechanics and Rock Engineering*, 50 (2017), 12, pp. 3121-3140
- [4] Hou, Z., *et al.*, Mechanical Behavior of Shale at Different Strain Rates, *Rock Mechanics and Rock Engineering*, 52 (2019), 10, pp. 3531-3544
- [5] Lora, R.V., *et al.*, Geomechanical Characterization of Marcellus Shale, *Rock Mechanics and Rock Engineering*, 49 (2016), 9, pp. 3403-3424
- [6] Wang, G., *et al.*, Experimental Study on the Anisotropic Mechanical Properties of Oil Shales Under Real-Time High-Temperature Conditions, *Rock Mechanics and Rock Engineering*, 54 (2021), 12, pp. 1-19
- [7] Yang, S. Q., *et al.*, Permeability Evolution Characteristics of Intact and Fractured Shale Specimens, *Rock Mechanics and Rock Engineering*, 50 (2021), 7, pp. 6057-6076
- [8] Yan, C., *et al.*, Mechanical Properties of Gas Shale During Drilling Operations, *Rock Mechanics and Rock Engineering*, 50 (2017), 7, pp. 1753-1765
- [9] Wu, S., *et al.*, Investigating the Propagation of Multiple Hydraulic Fractures in Shale Oil Rocks Using Acoustic Emission, *Rock Mechanics and Rock Engineering*, 55 (2022), 10, pp. 6015-6032
- [10] Mandal, P. P., *et al.*, Triaxial Deformation of the Goldwyer Gas Shale at In Situ Stress Conditions – Part I: Anisotropy of Elastic and Mechanical Properties, *Rock Mechanics and Rock Engineering*, 55 (2022), 10, pp. 6121-6149
- [11] Nezhad, M. M., *et al.*, Experimental Study and Numerical Modelling of Fracture Propagation in Shale Rocks During Brazilian Disk Test, *Rock Mechanics and Rock Engineering*, 51 (2018), 6, pp. 1755-1775
- [12] Jiang, F. J., *et al.*, The Main Progress and Problems of Shale Gas Study and the Potential Prediction of Shale Gas Exploration (in Chinese), *Earth Science Frontiers*, 19 (2012), 2, pp. 198-211
- [13] Cai, M., *et al.*, Generalized Crack Initiation and Crack Damage Stress Thresholds of Brittle Rock Masses Near Underground Excavations, *International Journal of Rock Mechanics and Mining Sciences*, 41 (2004), 5, pp. 833-847
- [14] Lu, H. J., *et al.*, Mechanical Behavior Investigation of Longmaxi Shale under High Temperature and High Confining Pressure, *Thermal Science*, 23 (2019), 3A, pp. 1521-1527
- [15] Huang, J., *et al.*, Shale Gas Accumulation Conditions and Favorable Zones of Silurian Longmaxi Formation in South Sichuan Basin (in Chinese), *Journal of China Coal Society*, 37 (2012), 5, pp. 782-787
- [16] Guo, J. C., *et al.*, A New Method for Shale Brittleness Evaluation, *Environmental Earth Sciences*, 73 (2015), 10, pp. 5855-5865
- [17] Martin, C. D., Chandler, N. A., The Progressive Fracture of Lac Du Bonnet Granite, *International Journal of Rock Mechanics and Mining Sciences and Geomechanics Abstracts*, 31 (1994), 6, pp. 643-659
- [18] Xie, H. P., *et al.*, Energy Mechanism of Deformation and Failure of Rocks (in Chinese), *Chinese Journal of Rock Mechanics and Engineering*, 27 (2008), 9, pp. 1729-1740